

DETECTION OF EVOLVED HIGH-REDSHIFT GALAXIES IN DEEP NICMOS/VLT IMAGES

NARCISO BENÍTEZ, TOM BROADHURST, RYCHARD BOUWENS

Astronomy Department, University of California, Berkeley, CA 94720

JOSEPH SILK

Astronomy and Physics Departments, and Center for Particle Astrophysics, University of California, Berkeley, CA 94720

&

PIERO ROSATI

European Southern Observatory, D-85748, Garching, Germany

Draft version January 18, 2018

ABSTRACT

A substantial population of high redshift early-type galaxies is detected in very deep UB-VRIJHK images towards the HDF-South. Four elliptical profile galaxies are identified in the redshift range $1 < z < 2$, with very red SEDs, implying ages of $\gtrsim 2$ Gyrs for standard passive evolution. We also find later type IR-luminous galaxies at similarly high redshift, (10 objects with $z > 1$, $H < 25$), with weak UV emission implying single burst ages of $\gtrsim 1$ Gyr. The number and luminosity-densities of these galaxies are comparable with the local E/SO-Sbc populations for $\Omega_m > 0.2$, suggesting that the major fraction of luminous Hubble-sequence galaxies have evolved little since $z \sim 2$. A highly complete photometric redshift distribution is constructed to $H = 25$ (69 galaxies) showing a broad spread of redshift, peaking at $z \sim 1.5$, in reasonable agreement with some analyses of the HDF. Four ‘dropout’ galaxies are detected at $z \approx 3.8$, which are compact in the IR, ~ 0.5 kpc/h at rest 3500\AA . No example of a blue IR luminous elliptical is found, restricting the star-formation epoch of ellipticals to $z \geq 10$ for a standard IMF and modest extinction.

Subject headings: galaxies: evolution

1. INTRODUCTION

The detection of early type galaxies at $z > 1$ requires deep IR imaging to overcome the observed large rest-frame optical K-correction and correspondingly minimal inferred passive spectral evolution for this class of galaxy (e.g. Stanford, Eisenhardt & Dickinson 1998). The highest redshift example of an early-type galaxy is a luminous object reported by Dunlop et al. (1996) at $z = 1.55$. Its restframe UV spectrum is dominated by late-type F-stars, equivalent to an age of ≈ 3 Gyrs, for standard stellar synthesis models (Spinrad et al. 1997). Following ordinary ellipticals to $z > 1$ requires much deeper IR imaging now possible from space. The NICMOS observation in the Hubble Deep Field South (Fruchter et al 1999) represents a three magnitude increase in depth over the deepest ground based IR data, and with usefully high spatial resolution. This, in combination with deep optical images from the VLT allows easy identification of red L^* ellipticals to $z \sim 2.5$, where significant spectral and density evolution is widely anticipated.

In section §1 we briefly outline our spectral and pro-

file fitting procedures and simulations as applied to the NICMOS and VLT observations. In §2 we discuss detections of early-type and other IR bright galaxies at high-redshift. In §3 we compare their statistical properties with local populations of Hubble sequence galaxies of similar spectral type, for different evolutionary models. In §4 we briefly discuss the absence of bright blue precursor ellipticals in the IR.

2. PHOTOMETRY, REDSHIFT ESTIMATION AND PROFILE FITTING

Three sets of images are utilized, the HDF-S NICMOS observations in JHK (Fruchter et al. 1999), the higher resolution unfiltered HST STIS image (Gardner et al. 1999) and the VLT Test Camera images in UBVRI (Fontana et al. 1999). We use the NICMOS pipeline zero-points and have computed the VLT effective zero-points for the combined optical images from the ESO photometric solution. The filter functions and instrument response curves are kindly made available by ESO and STScI. The detection is performed using SExtractor (Bertin & Arnouts 1996)

in a combined $J + H$ frame. Near total magnitudes are measured in J,H,K and PSF matched STIS images within a matched aperture set. A total of ≈ 200 galaxies are detected to $H=27$ within the central $50'' \times 50''$ field. The VLT UBVRI images have PSF's ≈ 3 times wider than the NICMOS exposures, and require a different procedure. We measure magnitudes within a $0''.9$ aperture and correct them to near-total magnitudes using versions of the $J + H$ band image degraded to the PSF of each of the VLT passbands to ensure the colors are defined within the same apertures for all bands.

Photometric redshifts are estimated using the methods described in Benítez (1999). The empirical template set of Coleman, Wu, & Weedman (1980) is used, and augmented with bluer local starbursts (Kinney et al. 1996), to determine the redshift probability distribution for each galaxy with Bayesian weighting. The fraction of objects with highly reliable photometric redshifts ($p>0.99$) is 57/69 to $H<25$ (24/25 for objects classified as earlier than Scd). Fainter than this magnitude limit the reliability of the photometric redshift estimates quickly degrades. We also allow for the quoted 10% uncertainty in the NICMOS zero-points for our spectral fits.

For redder early types, more detailed fits to single burst synthetic models are justified to accommodate the known spread of metallicity and age. For this, the compilation of Leitherer et al. (1996) is used, including the synthetic galaxy spectra of Bruzual & Charlot (1993). We also check that the colors of these objects are not compatible with dust reddened star-forming galaxies by generating reddened versions of the late and Im types in our template set.

Profile fitting is performed for bright galaxies in the IR ($H<23.7$). For this we simulate NICMOS images using the methods described in Bouwens, Broadhurst & Silk (1998) to account for the pixelization, dithering and point spread functions and the available weight map for the NICMOS dithering pattern.

3. HIGH-REDSHIFT RED GALAXIES

The $H < 25$ sample contains five clear elliptical galaxies, of which four lie above $z=1$. Their SED's and surface brightness profiles are compared with the models in Fig 1 and listed in Table 1. All the objects spectrally classified as ellipticals are also found to have spheroidal profiles (Fig 1). The most impressive object (NIC3/ET4, Fig 1, Table 1) is extremely red, consistent with minimal passive evolution at an estimated $z = 1.94 \pm 0.15$, with a clear de-Vaucouleurs profile and uniform color over its surface (~ 300 pixels). The effective radius $1.6(2.2)\text{kpc}/\text{h}$ is consistent with its inferred luminosity $M_{AB} = -21.96(-22.6)$ in restframe R for $\Omega_m = 1(0.1)$ (Binggelli, Sandage

& Tarenghi 1984). This IR conspicuous object is absent or only marginally detected in the U,B,V,R,I and STIS bands (Fig 1). Dust reddened spectra extinguished with standard reddening (Calzetti, Kinney, & Storchi-Bergmann 1994) are unable to generate the steep break from the relative flat IR. Another elliptical identified at $z = 1.66 \pm 0.25$ (NIC3/ET3, Fig 1, Table1) with a clear de-Vaucouleurs profile, is the luminous object reported by Treu et al. (1998) in the earlier NICMOS test images and confirmed by Stiavelli et al. (1999).

We also find several IR-bright high-redshift galaxies of later spectral type, 10 objects with $z>1$ and $H<25$. Two typical examples are shown in Fig 1. The profiles of these objects are generally exponential. The SED's are very conspicuous with a turn up towards the UV, and a distinctive bump in the IR separated by a trough, so there is little uncertainty in redshift (e.g. Fig 1). The best fit single burst minimum ages are typically ~ 1 Gyr. Comparison with the SEDs of CWW show these objects span the spectral types of local Sab to Sbc galaxies. The full sample of 24 galaxies with $H<25$ (open histogram, Fig 2) have a redshift distribution peaked at $z \sim 1.5$ with high- z tail similar to that found for the HDF (Connolly et al. 1997, Fernández-Soto, Lanzetta & Yahil 1998, Benítez 1999).

4. DENSITY EVOLUTION

A reliable measurement of the space density of massive galaxies at high redshift provides a basic check of hierarchical models of galaxy formation, where the most massive haloes form late (Lacey & Cole 1993) and in which ellipticals and massive spheroids may be viewed as the end product of the merging of smaller systems.

The presence of so many luminous red galaxies at high- z in such a small field is surprising and indicates that relatively evolved luminous galaxies are commonplace at $z>1$. Using the Pozzetti, Bruzual, & Zamorani (1996) local luminosity functions for E/SO-Sbc as input, we recover 4(9) ellipticals from our realistic NICMOS simulations for $z > 1$, $H < 25$, with $\Omega_m = 1(0.2)$ and no evolution. Adding the later-type IR-luminous galaxies allows a useful comparison with models (Fig 2). The redshifts and luminosities observed above $z=1$ are consistent with no density or luminosity evolution of standard Hubble sequence galaxies for $0.2 < \Omega_m < 1$. Note, passive evolution is minimized here for consistency with the red SEDs by choosing $H_0 = 50\text{km/s/Mpc}$ and $z_f = 15$. The hierarchical model parametrization of Kauffmann, Charlot & White (1996) for $\Omega = 1$ underpredicts the numbers as expected. Hierarchical models with $\Omega < 1$ may allow a declining density but must be checked

for self consistency. The optical-IR colors prefer older higher redshift models and are consistent with no size evolution, but do not distinguish clearly between the above cosmological models.

The integrated luminosity density to $H=25$ at $1 < z < 2.5$ is comparable with local estimates integrated over E/SO-Sbc types (see Fig 2). The predicted luminosity density for $z > 1$ at rest-frame 6000Å is 4.3×10^{19} ergs/cm²/s/Hz compared to $3.9 \pm 1.4 \times 10^{19}$ ergs/cm²/s/Hz, $2.41 \pm 0.9 \times 10^{19}$ ergs/cm²/s/Hz and $2.06 \pm 0.8 \times 10^{19}$ ergs/cm²/s/Hz, for $\Omega_m = 1$, $\Omega_m = 0.1$ and $\Omega_m + \Omega_\Lambda = 0.25 + 0.75$ respectively. A factor of two decrease in luminosity density is implied relative to the popular low Ω_m models assuming passive or no stellar evolution.

Our results seem to extend to $z \approx 2$ the results of other authors notably Lilly et al. (1995) and Kodama, Bower & Bell (1999) who find no evidence for a dramatic evolution in the density of early types galaxies to $z \sim 1$. The contrast of our results with the absence of distant ellipticals claimed by others (Kauffmann & Charlot 1998; Zepf 1997; Franceschini et al. 1996; Barger et al. 1998; Menanteau et al. 1998) can be put in context by appreciating that the NICMOS data is complete to $H \approx 27$, which is 3 magnitudes fainter than the deepest ground based data and 6 magnitudes fainter than most work on this question. Two of the four ellipticals found here in the IR would barely register in the I band ($I \sim 27$) and are certainly not bright enough for morphological classification in the optical even from space. Recent claims of a decline in the elliptical density for $z > 1$ rely on significant passive evolution, where brightening enhances the expected numbers. The claim by Kauffmann, Charlot, & White (1996), based on the CFRS (Lilly et al. 1995) is subject to redshift incompleteness, in particular of red high-z galaxies, which are very hard to measure spectroscopically. Some of the red galaxies reported here are bright enough in the IR to be detected in previous deep Keck images (Moustakas et al. 1997; Hogg et al. 1997) but morphological classification is not possible in ground based images and deep complementary optical data are required to establish the break. The NICMOS images directly show that luminous early type galaxies are present in significant numbers at high redshift with SEDs too red to be recognized as ellipticals in the optical even in the deepest WFPC2 images.

An obvious problem with this kind of work is the presence of clustering in small field, rendering the results uncertain. To explore this we have searched for spikes in the redshift distribution using the approach described in Benítez (1999). The minimal number of structures along the light-of-sight to $H=25$ is three, at $z = 0.55$ (consistent with the 0.58 redshift spike

found in the HDF-S by Glazebrook et al. 1999), $z = 1.35$ and $z = 1.95$. Each of these structures corresponds approximately to the redshift of one or more elliptical galaxies, and the two higher redshift peaks contain $\approx 1/3$ of all the $z > 1, H < 25$ galaxies. Our statistical analysis shows that it is virtually impossible that all the early type galaxies at $1 < z \lesssim 2$ belong to a single spike. A rough estimate of the expected clustering noise can be obtained by integrating the faint galaxy correlation function over the NICMOS field for the range $1 < z < 2$. Connolly, Szalay & Brunner 1998 measure an amplitude $A(10'') = 0.12(\omega \propto \theta^{-0.8})$ for the angular correlation of HDF-N galaxies within $\Delta z = 0.4$ slices to $z \sim 1.5$. Assuming that $A \propto 1/\Delta z$, the total variance in the number of galaxies in a redshift slice Δz is $\sigma^2(\Delta z) \sim N(\Delta z)[1 + N(\Delta z)(0.4/\Delta z)0.07]$. For the interval $1 < z < 2$ with 35 galaxies this yields a variance of $\sigma = 8.3$ galaxies, which is 40% greater than Poisson. If the early types are clustered like the integral of all types then we estimate their number to be 14 ± 4 in the range $1 < z < 2$.

5. VERY HIGH-REDSHIFT BLUE GALAXIES

The lack of spectral evolution of early type galaxies demonstrates that star-formation does not extend over time, but is confined to an early brief period, so that we should expect the precursors of these galaxies to appear extremely luminous and blue at higher redshift. The width of this period is constrained to be short by the tight E/SO color-magnitude and M/L sequences (e.g. Bower, Lucey & Ellis 1992, Van-Dokkum et al. 1998). More directly, the lack of blue ellipticals in the HDF (e.g. Franceschini et al. 1998) means this epoch lies at $z > 5$, and therefore may appear in the near-IR for redshifts in range $5 < z < 15$ as I or J band ‘dropouts’, provided the IMF of early-type galaxies is not unusually deficient in hot stars.

Our simulated NICMOS images show that significant numbers of elliptical galaxies are expected in the IR if they form luminous stars high redshift and were not significantly extinguished during the first Gyr. The simulations include an exponential burst at $z_f = 15$ with an e-folding time of 1Gyr and predicts 6, 10 and 15 objects for $z > 5$ to $H=26$ for, $\Omega_m = 1$, $\Omega = 0.1$, $\Omega_m + \Omega_\Lambda = 0.25 + 0.75$. In comparison, no I or J band ‘dropout’ galaxies are observed brighter than this limit.

At lower redshift, five compact optically blue dropout galaxies are found, all consistent with a single redshift of $z \approx 3.8$. Fits to their spectra are shown in Fig 3. These objects have low SFR of $6-23 M_\odot/yr$ and very compact sizes in the H-band, ~ 0.5 kpc/h at restframe 3500Å ($\Omega_m=1$), and therefore appear unlikely to be the precursors of luminous elliptical

galaxies if no evidence of SF is to remain by $z \sim 1$.

6. CONCLUSIONS

We have detected a substantial population of early type galaxies at $z > 1$. These include $r^{1/4}$ profile galaxies in the redshift range $z > 1$, all of which have surprisingly red colors despite their large redshifts. Later spectral-types are also present in this redshift range, with a conspicuous IR bump. These galaxies are all luminous and well evolved, with minimum single-burst ages > 1 Gyr for a standard IMF.

The clear detection of early type galaxies and spheroidal components of other high- z disk galaxies points to the existence of a roughly similar density of luminous Hubble sequence galaxies at $z \sim 2$, compared to the local Universe. The declining density of luminous galaxies expected in hierarchical schemes can be made consistent with the data only with for

low Ω_m models. Low Ω_m helps accommodate the absence of spectral evolution, but in any cosmology the lack of bright IR-blue precursors of elliptical galaxies requires a very high redshift of formation $z > 10$, for a standard IMF and extinction.

Although the field studied is small, the number of red high- z galaxies detected is surprising and strongly suggests that the bulk of luminous galaxies were formed at $z \gtrsim 2$. In the short-term a deep NICMOS pointing in the HDF will provide similar data and help average over clustering. Progress on this question awaits deep diffraction-limited IR imaging on large telescopes and improved IR facilities in space.

We would like to thank Bob Williams and the Hubble Deep Field South Team as well as Alvio Renzini and the VLT-UT1 Science Verification Team for making available this useful data.

REFERENCES

Barger, A. J., et al. 1998, *ApJ*, 501, 522
 Benítez, N. 1999, submitted to *ApJ*, astro-ph/9811129.
 Bertin, E., & Arnouts, S. 1996, *A&AS*, 117, 393.
 Binggeli, B., Sandage, A., & Tarenghi, M. 1984, *ApJ*, 89, 64.
 Bower, R.G., Lucey, J.R., & Ellis, R.S. 1992, *MNRAS*, 254, 601
 Bouwens, R.J., Broadhurst, T.J., & Silk, J. 1998, *ApJ*, 506, 557.
 Bruzual A., G. & Charlot, S. 1993, *ApJ*, 405, 538
 Calzetti, D., Kinney, A.L., Storchi-Bergmann, T. 1994, *ApJ*, 429, 582.
 Coleman, G.D., Wu, C.-C., & Weedman, D.W. 1980, *ApJS*, 43, 393.
 Connolly, A. J., Szalay, A. S., Dickinson, M., Subbarao, M. U., & Brunner, R. J. 1997, *ApJ*, 486, L11
 Connolly, A. J., Szalay, A. S. & Brunner, R. J. 1998, *ApJ*, 499, L125
 Dunlop, J., Peacock, J., Spinrad, H., Dey, A., Jimenez, R., Stern, D., & Windhorst, R.A. 1996, *Nature*, 381, 581.
 Fernández-Soto, A., Lanzetta, K.M. & Yahil, A. 1998, to appear in *ApJ*, astro-ph/9809126
 Fontana, A., D'Odorico, S., Fosbury, R., Giallongo, E., Hook, R., Poli, F., Renzini, A., Rosati, P., & Viegzer, R. 1999, to appear in *A&A*, astro-ph/9901359
 Franceschini, A., Silva, L., Fasano, G., Granato, L., Bressan, A., Arnouts, S., & Danese, L. 1998, *ApJ*, 506, 600
 Fruchter et al. 1999, to appear in *AJ*
 Gardner et al. 1999, to appear in *AJ*
 Glazebrook et al. 1999, in preparation
 Hogg, D. W., Neugebauer, G., Armus, L., Matthews, K., Pahre, M. A., Soifer, B. T., & Weinberger, A. J. 1997, *AJ*, 113, 2338
 Kauffmann, G. 1996, *MNRAS*, 281, 487.
 Kauffmann, G. & Charlot, S. 1998, *MNRAS*, 297, L23.
 Kauffmann, G., Charlot, S., & White, S.D.M. 1996, *MNRAS*, 283, L117.
 Kinney, A.L., Calzetti, D., Bohlin, R.C., McQuade, K., Storchi-Bergmann, T., & Schmitt, H.R. 1996, *ApJ*, 467, 38.
 Kodama, T., Bower, R.G. & Bell, E.F. 1999, submitted to *MNRAS*, astro-ph/9810138
 Lacey, C. & Cole, S. 1993, *MNRAS*, 271, 676
 Leitherer, C., et al. 1996, 108, 996.
 Lilly, S.J., Tresse, L., Hammer, F., Crampton, D., & Le Févre, O. 1995, *ApJ*, 455, 108
 Madau, P., Pozzetti, L., & Dickinson, M. 1998, *ApJ*, 498, 106
 Menanteau, F., Ellis, R.S., Abraham, R.G., Barger, A.J. & Cowie, L.L., submitted to *MNRAS*, astro-ph/9811465
 Moustakas, L. A., Davis, M., Graham, J. R., Silk, J., Peterson, B. A., & Yoshii, Y. 1997, *ApJ*, 475, 445
 Pozzetti, L., Bruzual, G. & Zamorani, G. 1996, *MNRAS*, 281, 953.
 Spinrad, H., Dey, A., Stern, D., Dunlop, J., Peacock, J., Jimenez, R., & Windhorst, R. 1997, *ApJ*, 484, 581.
 Stanford, S.A., & Eisenhardt, P.R., & Dickinson, M. 1998, *ApJ*, 492, 461.
 Stiavelli, M., et al. 1999, submitted to *A&A*, astro-ph/9812102.
 Treu, T., et al. 1998, *A&A*, 340, L10
 Van Dokkum, P. G., Franx, M., Kelson, D. D., & Illingworth, G. D. 1998, *ApJ*, 504, L17
 Zepf, S. 1997, *Nature*, 390, 377.

TABLE 1
 $z > 1$ EARLY TYPE GALAXIES IN THE HDF/NIC3 FIELD

name	X	Y	$m_{F160W,AB}$	z_{phot}	r_{hl}	$STIS_{AB} - F160W_{AB}$	Age(Gyr)
NIC3/ET1	181.6	868.87	21.24 ± 0.01	1.41 ± 0.20	$0''.34$	3.3	> 1.5
NIC3/ET2	439.2	352.34	24.50 ± 0.06	1.55 ± 0.20	$0''.31$	> 4.0	> 1.5
NIC3/ET3	607.4	371.52	21.79 ± 0.01	1.66 ± 0.25	$0''.26$	4.2	> 2
NIC3/ET4	646.8	898.32	23.18 ± 0.02	1.94 ± 0.15	$0''.39$	> 5.4	> 3.5

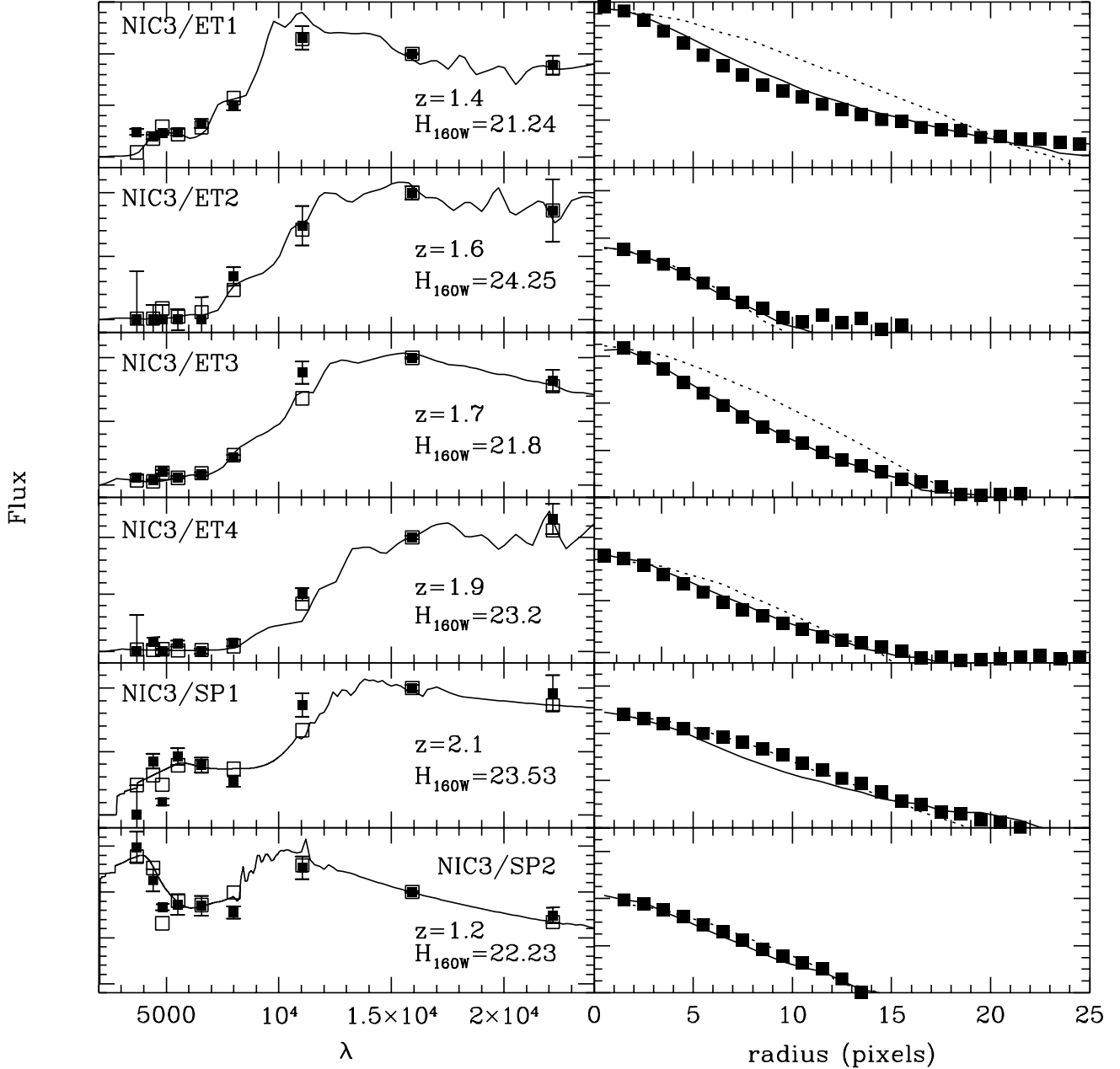


FIG. 1.— The left panel shows our best fit elliptical galaxies at $z>1$. On the left is the SED fit to the multiband photometry where the data points should be compared with the integrated flux over the passband from the best fit model and represented as open squares. The corresponding model spectrum is also shown. On the right are the convolved exponential (dotted) and de-Vaucouleurs (solid) best fits to the data, plotted as log surface-brightness versus linear radius for clarity. The two lower panels are representative examples of later spectral types at high redshift (Sab and Sbc), demonstrating the utility of U through K broadband information for identifying redshifts of these galaxy types at high redshifts. The positions of objects ET1 through ET4 are listed on Table1; objects SP1 and SP2 have coordinates (595.8, 1001.3) and (835.4, 1022.2).

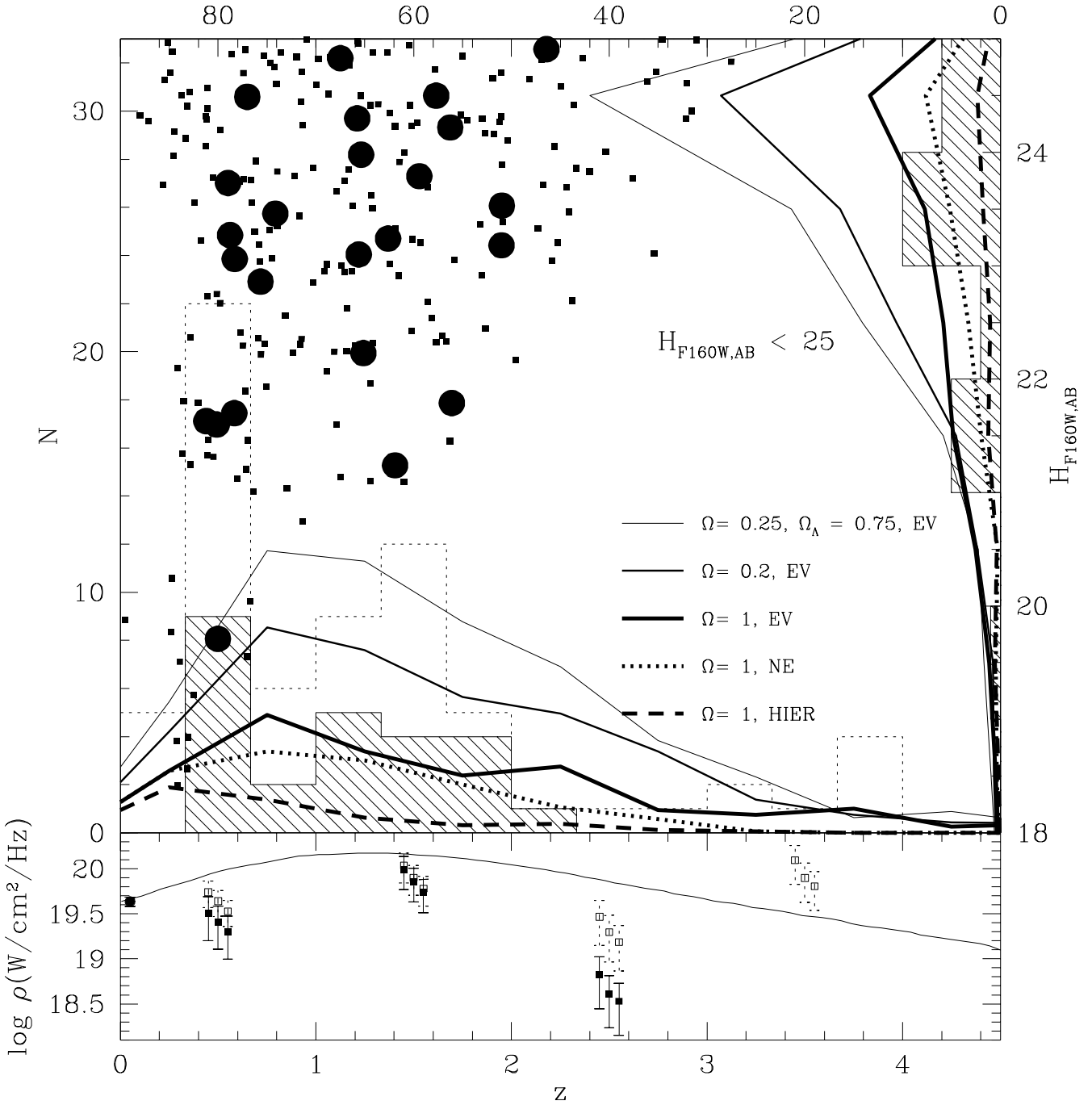


FIG. 2.— Models of local E/SO-Sbc luminosity functions recovered from simulated images matched to the properties of the NICMOS South data. These are compared with the redshift distribution of E/SO-Sbc spectral types to $H = 25$ in the lower histogram and against apparent magnitude to the left. The predicted range of redshifts is similar to the data (shaded histogram) for all models, but the observed numbers are greater than expectations of hierarchical models for massive galaxies with $\Omega_m = 1$ and underpredict no-evolution or mild passive evolution with larger volume cosmologies. Consistency is found with mild or no stellar evolution for relatively flat Ω_m dominated models. Several Monte-Carlo realizations of the redshift-magnitude distribution for a no-evolution $\Omega = 1$ model (small points) are compared to the observations (big points). Dotted histograms give the redshift distribution for all types to $H = 25$. The lower panel shows the luminosity density with redshift for the spectrally early-type galaxies (solid squares) and for the whole sample (open squares) to $H = 25$ at rest 6000Å. Compared with the local luminosity-density of E/SO-Sbc galaxies (left most point), there is no obvious trend. The curve is our calculation of the luminosity density at rest 6000Å using the Madau, Pozzetti & Dickinson (1998) SF history for the Salpeter IMF and no dust.

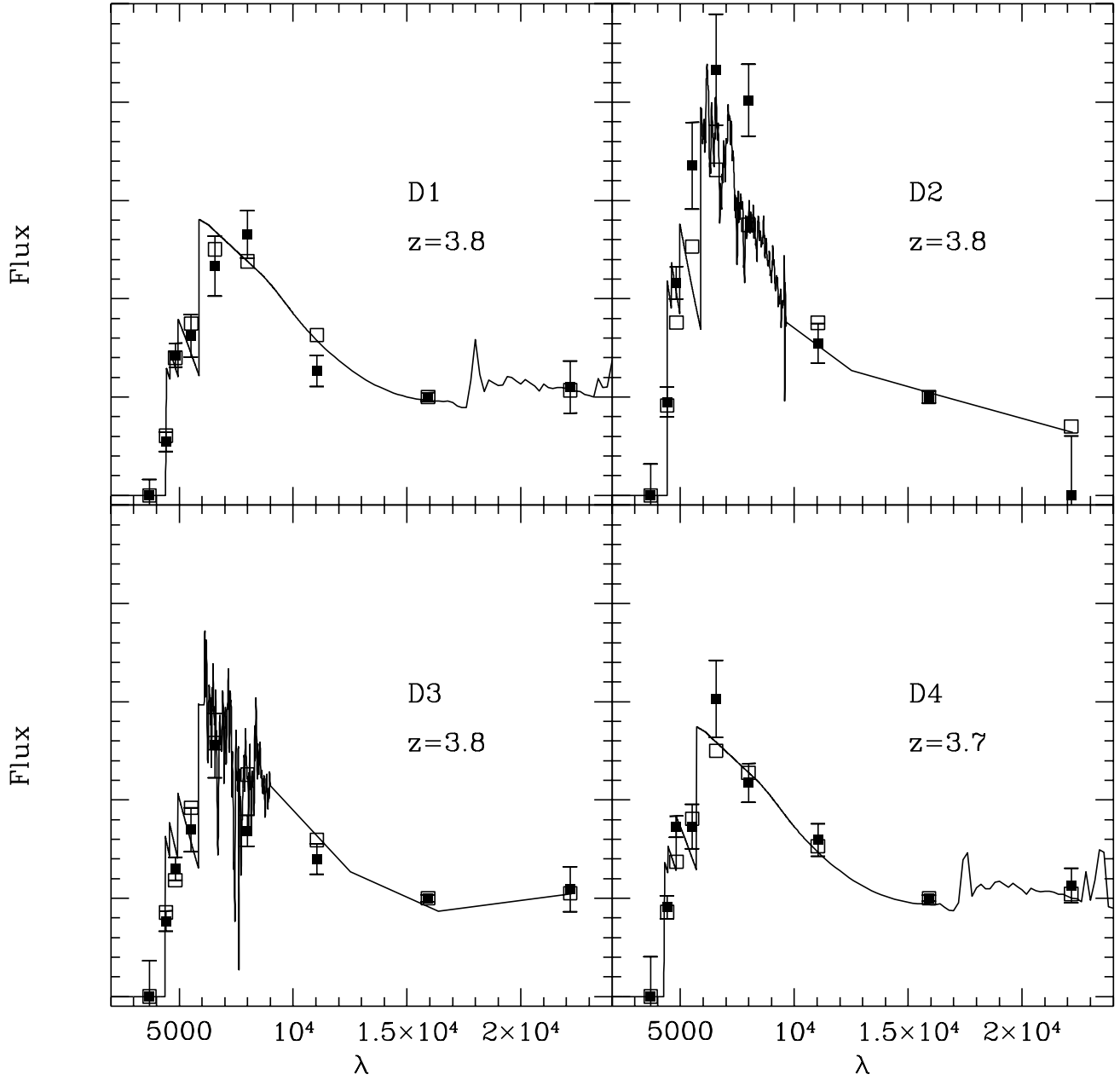


FIG. 3.— The optical dropout galaxies showing the best single burst minimum ages ranging from 10^6 - 10^8 yrs and star formation rates of between 6 - $23 M_{\odot}/\text{yr}$ for a Salpeter IMF and $\Omega = 1$. These blue objects are very compact in the IR ~ 0.5 kpc/h at rest 3500\AA and all consistent with lying at $z \approx 3.8$. No example of a higher redshift IR-dropout galaxy up to $H < 26$ is found, placing a useful constraint on single burst models of luminous galaxy formation (see text). D1,D2,D3 and D4 have respectively positions (244.3, 598.1), (318.3, 855.7), (857.6, 847.4) and (497.8, 770.7)